3406 © 1983 The Chemical Society of Japan Bull. Chem. Soc. Jpn., 56, 3406—3409 (1983) [Vol. 56, No. 11

Structure of Liquid *N*,*N*-Dimethylformamide Studied by Means of X-Ray Diffraction

Hitoshi Ohtaki,* Sumiko Itoh, Toshio Yamaguchi, Shin-ichi Ishiguro
and B. M. Rode†

*Department of Electronic Chemistry, Tokyo Institute of Technology at Nagatsuta,
4259 Nagatsuta-cho, Midori-ku, Yokohama 227*

†*Institute of Inorganic and Analytical Chemistry, University of Innsbruck,
Innrain 52a, A-6020 Innsbruck, Austria*

(Received July 16, 1983)

The structure of *N*,*N*-dimethylformamide (DMF) was determined at 25 °C by means of X-ray diffraction using a θ-θ type X-ray diffractometer. The least-squares analysis of the reduced intensities results that a DMF molecule has a practically planar skeletal structure in the liquid state. Intramolecular structural parameters within a DMF molecule were determined as follows: C=O; 1.24 Å, N-C(CHO); 1.35 Å, and N-C(CH_3); 1.45 Å. The bond lengths are not appreciably different from those found in the gas phase, except for the C=O length, which is slightly longer by 0.04 Å in the liquid state than in the gaseous one. The radial distribution curve of DMF shows that the intermolecular arrangement of DMF molecules is practically fully disordered and no evidence has been found for the cluster formation of DMF molecules in the liquid state. The experimental result for the weak intermolecular interactions between DMF molecules is supported by *ab initio* MO-SCF calculations.

Structural studies of liquid amides have drawn considerable attentions of physical chemists and biochemists in connection with the conformation of amide moieties in polypeptides.[1–3] The structure of formamide has been extensively investigated in the liquid state,[4–9] as well as in the gaseous[10] and solid[11,12] phases. Theoretical considerations have also been carried out for the structure of formamide.[13,14] The molecular structure of *N*,*N*-dimethylformamide (DMF) has been determined in the gas phase by electron diffraction[15] and microwave[16] methods and they concluded that all atoms except hydrogen atoms at the methyl groups lay on one plane. The structure of DMF in the solid state has been studied for crystalline solvates,[17–19] but no crystal structure has been determined for pure DMF. Theoretical treatments for the molecular structure of DMF have also been done by some authors[2,20] for the electron distribution on the atoms within the DMF molecule. However, intermolecular interactions between DMF molecules have not been taken into the theoretical consideration.

Raman and infrared spectra of liquid DMF have been recorded by Fini and Mirone,[21] from which they concluded that DMF molecules formed clusters oriented in a partially ordered way. However, the cluster formation has not been conclusive from NMR measurements.[22–26] No X-ray study has been carried out so far for the structure of liquid DMF.

Since X-ray diffraction measurements can provide direct information for ordered structures of liquids, we aimed at investigating the liquid structure of DMF and comparing it with the structure of formamide examined in a previous work.[9]

Experimental

Reagents. Commercially available *N*,*N*-dimethylformamide of analytical grade was dried with Molecular Sieves (4A) and then distilled under a reduced pressure.

Method of Measurements and Analysis of Scattering Data. A sample solution was placed in a flat glass tray of 38 mm depth. X-Ray scattering measurements were carried out at (25±2) °C in a thermostatted room by using a JEOL θ-θ diffractometer with a bent LiF monochromator. Mo $K\alpha$ radiation (λ=0.7107 Å) was used. The scattered intensities were collected at discrete points over the s-range from 0.6 Å^{-1} to 16.4 Å^{-1} ($s=4\pi\lambda^{-1}\sin\theta$, where 2θ is the scattering angle). Details of the method of measurements have been described elsewhere.[27]

Experimental intensity data were corrected for background, absorption, double scattering, polarization and incoherent scatterings by the usual methods and then normalized to the absolute scale with respect to a stoichiometric unit volume V containing one DMF molecule.

The radial distribution curve was calculated by using a Fourier transform

$$D(r) = 4\pi r^2\rho_0 + 2r\pi^{-1}\int_{s_{\min}}^{s_{\max}} s\cdot i(s)\cdot M(s)\cdot \sin(sr)\mathrm{d}s, \qquad (1)$$

were ρ_0 denotes the average scattering density, $M(s)$ a modification function of the form $[\sum \mathrm{n}_i\{(f_i(0)+\Delta f_i')^2+(\Delta f_i'')^2\}/\sum \mathrm{n}_i\{(f_i(s)+\Delta f_i')^2+(\Delta f_i'')^2\}]\cdot\exp(-0.01s^2)$. The $s_{\min}$ and $s_{\max}$ values are 0.6 Å^{-1} and 16.4 Å^{-1}, respectively. The reduced intensities $i(s)$ were given as follows:

$$i(\mathrm{s}) = I(s)_{\mathrm{obsd}} - \sum \mathrm{n}_i\{(f_i(s)+\Delta f_i')^2+(\Delta f_i'')^2\}, \qquad (2)$$

and n_i is the number of atom i in the stoichiometric volume and $f_i(s)$ denotes the scattering factor of atom i at s. $\Delta f_i'$ and $\Delta f_i''$ are the real and imaginary parts of anomalous dispersion of atom i, respectively.

Theoretical reduced intensities were calculated by Eq. 3:

$$\begin{aligned} i(s) = {} & \sum \mathrm{n}_j[\sum n_{pq}\{(f_p(s)+\Delta f_p')(f_q(s)+\Delta f_q') \\ & +\Delta f_p''\Delta f_q''\}\cdot\frac{\sin(sr_{pq})}{(sr_{pq})}\cdot\exp(-b_{pq}s^2)] \\ & -\frac{4\pi R_j^3}{3V}\cdot\frac{3\{\sin(sR_j)-sR_j\cos(sR_j)\}}{(sR_j)^3} \\ & \cdot\exp(-B_js^2)\cdot\{\sum \mathrm{n}_i(f_i(s)+\Delta f_i')\sum \mathrm{n}_j\cdot \\ & (f_j(s)+\Delta f_j')+\sum \mathrm{n}_i\Delta f_i''\sum \mathrm{n}_j\Delta f_j''\}, \end{aligned} \qquad (3)$$

where r_{pq}, b_{pq}, and n_{pq} stand for the distance, the temperature factor, and the frequency factor of the p-q atom-pair, respectively. R_j denotes the distance from an atom j beyond which a continuous electron distribution is assumed. A parameter B_j is introduced since the emergence of such a

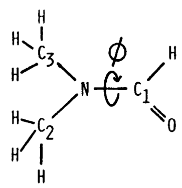

Fig. 1. The structure of DMF molecule.

continuous electron distribution around atom j is not sharp. Intramolecular interactions of all possible atom-pairs of DMF were calculated by using the first term of Eq. 3, while interactions between different molecules were approximated by using the second term of Eq. 3 on the assumption of the continuous electron distribution beyond the R_j values of each atom in one molecule. The R_j values were selected in order to obtain the best fit $s \cdot i(s)$ curve to the experimental one and assumed to be 2.50 Å for H and N atoms and 3.30 Å for O and C atoms by taking into consideration the interatomic distances found in the present work as will be shown later. The B_j values were set to be 0.05 Å^2 for all the atoms. The C–H bond length within a DMF molecule was fixed at 1.09 Å. The calculations were performed by using the KURVLR program.[28]

Distances of atom-pairs in the system were first assumed to be the same as those with the literature values reported from the electron diffraction measurement in the gas phase,[15] and then the structural parameters of the atom-pairs were refined by the least-squares method applied to the reduced intensities so as to minimize the error-square sum $U = \sum w\{i(s) - i(s)_{\mathrm{calcd}}\}^2$, where the weighting function $w = I(s)_{\mathrm{obsd}}^{-2} \cdot \cos\theta$. The NLPLSQ program was used for the calculations.[29]

For the sake of convenience of the discussion in the following section, we numbered the carbon atoms within a DMF molecule (Fig. 1).

Results and Discussion

The $s \cdot i(s)$ and radial distribution $(D(r) - 4\pi r^2 \rho_0)$ curves are shown in Figs. 2 and 3, respectively. The radial distribution curve of formamide is also shown in Fig. 3 for comparison.

Two distinct peaks are observed at 1.3 and 2.3 Å in the radial distribution curve of DMF (Fig. 3a). The former peak contains peaks due to the N–C$_1$, N–C$_2$, N–C$_3$, and C$_1$=O bonds within each DMF molecule, and the latter can be ascribed to the C$_1$···C$_2$, C$_1$···C$_3$, C$_2$···C$_3$, and N···O nonbonding interactions. No significant peak is found in the range $r > 3$ Å in the radial distribution curve of DMF, in contrast to that of formamide (see Fig. 3b).

NMR studies showed that a DMF molecule can rotate along the N–C$_1$ axis, although the free energy of activation of the rotation of the molecule is rather large (88 kJ mol^{-1}).[30] Therefore, we first attempted to postulate two possibilities of configuration of a DMF molecule; *i.e.*, a planar ($\phi = 0°$) and a perpendicular ($\phi = 90°$) structures (see Fig. 1). For the both model-structures we employed the least-squares calculation for the reduced intensities over the s-range from 3.5 Å^{-1} to 16 Å^{-1} in order to find structural parameters which can best reproduce the experimental $s \cdot i(s)$ values. In the course of the calculations we assumed a tetrahedral structure of the methyl groups within a DMF molecule and the C–H bond length to be 1.09 Å. The results obtained from the two models are compared with the experimental values in Fig. 2, and it is obvious that the planar model gives a much better fit to the experimental curve than the perpendicular one does. Moreover, when we introduced interatomic distances calculated from models at $\phi = 30°$ and 60° as the initial values and allowed them to be optimized without fixing the rotation angle, the distances converged to the values resulted from the least-squares analysis at $\phi = 0°$. Therefore, we concluded that the structure of a DMF molecule is practically planar. The final values of the bond distances thus obtained are listed in Table 1, together with the values found in the gaseous and solid states. The bond angles were estimated as follows: ∠N–C$_1$–O; (121±3)°, ∠C$_1$–N–C$_2$ = ∠C$_1$–N–C$_3$; (116±4)°, and ∠C$_2$–N–C$_3$; (124±5)°.

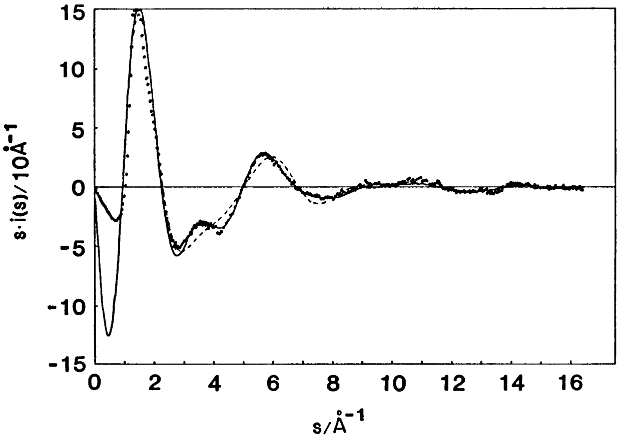

Fig. 2. The $s \cdot i(s)$ values of liquid DMF. Circles represent the $s \cdot i(s)$ values experimentally obtained. The solid line shows the theoretical $s \cdot i(s)$ values at $\phi = 0°$ including those for interactions between atoms and electrons continuously distributed in the region of $r > R_j$. The dashed line shows the theoretical values at $\phi = 90°$.

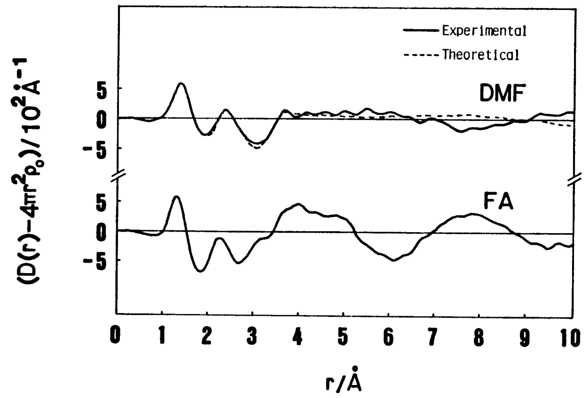

Fig. 3. Radial distribution curves $D(r) - 4\pi r^2 \rho_0$. (a) DMF. The solid and dashed lines represent experimental and theoretical curves, respectively. (b) Formamide.

The intramolecular bond distances of each atom-pair in DMF found in the liquid state are well consistent with those in the gas phase[15] except for the

Table 1. The intramolecular distances (r) and the temperature factors (b) of atom-pairs in liquid DMF. The values in parentheses are their standard deviations estimated (3σ). The bond lengths within a DMF molecule determined in the gas phase and in a crystalline solvate are also shown

Atom-pair	Gas[15) r/Å	Liquid r/Å	Liquid b/Å^2	Crystalline solvate[18) r/Å
C_1=O	1.20	1.24(1)	0.003(1)	1.30
N-C_1	1.34	1.35(2)	0.002(1)	1.28
N-C_2	1.45	1.45(1)	0.004(1)	1.51
N-C_3	1.45	1.45(1)	0.004(1)	1.50

C=O bond length, which is slightly longer by 0.04 Å in the liquid state than in the gaseous one. The result may indicate a weak hydrogen-bonded interaction between DMF molecules. However, there are some discrepancies in the bond distances between in the liquid state and in a crystalline solvate,[18) probably because of strong ion-DMF interactions in the crystalline solvate compared with intermolecular interactions of DMF themselves in the liquid state.

In the radial distribution curve of DMF we do not find appreciable peaks in the range $r>3$ Å, in which we see still peaks due to intermolecular interactions of formamide molecules (Fig. 3). If we assumed a continuous electron distribution beyond R_j from each atom j within a DMF molecule, the reduced intensities calculated from Eq. 3 gave values which fitted satisfactorily with the experimental ones over the wide s-range of 1 Å^{-1} to 16 Å^{-1} (see solid line in Fig. 2). The radial distribution curve showed no distinct peak beyond $r=3$ Å, which indicated a practically random distribution of molecules in the system. Therefore, the result indicated that no significant interactions existed between molecules through, for instance, hydrogen bonds and thus the cluster formation of DMF molecules was not observed from the present X-ray diffraction work.

However, it is obvious that DMF molecules interact with each other to form a condensed phase at a room temperature. Therefore, we estimated the interaction energy between DMF molecules with the aid of the *ab initio* MO-SCF method by using some suitable structure models and minimal basis sets. The geometry of the DMF molecules was fixed at the experimental one obtained by the present work, and the distance between DMF molecules and the configuration of DMF associates were varied. The calculations were performed in a similar way as described previously.[9)

The dimer model used for the calculation is shown in Fig 4. At $\Theta=\Theta'=180°$, the dimer at $\Psi=0°$ was more stable by *ca.* 8.4 kJ mol^{-1} than that at $\Psi=180°$ when the intermolecular C–H···O distance was 3.2 Å. In the latter configuration the lowest energy of interaction was found at $\Theta=180°$ and $\Theta'=90°$ at $r_{\text{C-H}\cdots\text{O}}=$ 3.2 Å. At $\Theta'=120°$ a slightly higher energy of stabilization was estimated for the dimer, but the difference was too small (*ca.* 1 kJ mol^{-1}) to be significant.

The rotation barrier of the DMF dimer around the

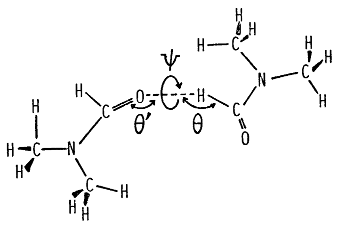

Fig. 4. The dimer model of DMF.

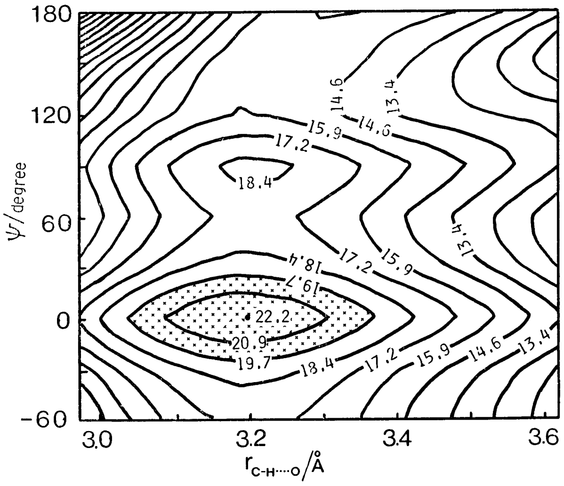

Fig. 5. The energy surface for the linear-dimer of DMF plotted against the C–H···O distance ($r_{\text{C-H}\cdots\text{O}}$) between molecules and the rotation angle Ψ around the C–H···O axis. The numbers indicated in the diagram show the stabilization energy of the dimer ($-\Delta E$) in kJ mol^{-1} units.

C–H···O axis at $\Theta=\Theta'=180°$ was calculated at various C–H···O distances. The energy surface diagram is plotted for varying bond distance $r_{\text{C-H}\cdots\text{O}}$ and rotation angle Ψ in Fig. 5. The numbers indicated in the diagram show stabilization energies of dimerization of DMF molecules ($-\Delta E$) in kJ mol^{-1} units. It is seen from the diagram that the configuration is most stable at $r_{\text{C-H}\cdots\text{O}}=3.2$ Å and $\Psi=0°$, but the curvature is so small that the bond distance and the rotation angle can change over the range ±0.15 Å and ±30°, respectively, by the thermal energy (kT) at $T=300$ K. The crosshatched area in Fig. 5 indicates the region where the variation of the energy is smaller than the kT value at room temperature. The maximum stabilization energy of dimerization was estimated to be -22.2 kJ mol^{-1} (see Fig. 5), which is much smaller than the energies of hydrogen bonds of water molecules (-30 to -40 kJ mol^{-1}) and of formamide (-68 kJ mol^{-1} [19)). The ring-dimer structure of DMF was much less stable than the linear dimer examined above.

A chain-trimer connected by the C–H···O hydrogen bonds of DMF molecules had a similar stabilization energy (-23 kJ mol^{-1}) per bond as the linear dimer, and thus, no special stabilization is to be expected by the formation of oligomers. The vibrational amplitude of the C–H···O bond at room temperature was estimated to be about 0.23 Å from the surface of the stabilization energy of the trimer and the kT value. The amplitude of the trimer is practically the same as that of the dimer (0.15 Å). Since the vibrational amplitude of DMF associates is fairly large, we may not expect to detect the associated species as discrete units in the liquid DMF. This conclusion is consistent with that obtained by the X-ray diffraction measurement demonstrated in the present study.

The present work has been financially supported by the Grant-in-Aid for Scientific Research (No. 57470054) from the Ministry of Education, Science and Culture. The Asahi Glass Foundation for Industrial Technology also financially supports the present work. The financial support by the Austrian Federal Ministry for Science and Research (Erl. Zl. 18.854/6—10/81) is also gratefully acknowledged.

References

1) E. B. Nielsen and J. A. Schellman, *J. Phys. Chem.*, **71**, 2297 (1967).

2) J. F. Yan, F. A. Momany, R. Hoffmann, and H. A. Scheraga, *J. Phys. Chem.*, **74**, 420 (1970).

3) J. Applequist, *J. Chem. Phys.*, **71**, 4324 (1979).

4) J. F. Hinton and K. H. Ladner, *J. Magn. Reson*, **6**, 586 (1972).

5) H. Siegbahn, L. Asplund, P. Kelfve, K. Harmin, L. Karlsson, and K. Siegbahn, *J. Electrosc. Relat. Phenom.*, **5**, 1059 (1974).

6) D. J. Gardiner, A. J. Lees, and B. P. Straughan, *J. Mol. Struct.*, **53**, 15 (1979).

7) R. J. DeSando and G. H. Brown, *J. Phys. Chem.*, **72**, 1088 (1968).

8) E. Kálmán, I. Serke, G. Pálinkás, M. D. Zeidler, F. J. Wiesmann, H. Bertagnolli, and P. Chieux, *Z. Naturforsch.*, *A*, **38**, 231 (1983).

9) H. Ohtaki, A. Funaki, B. M. Rode, and G. J. Reibnegger, *Bull. Chem. Soc. Jpn.*, **56**, 2116 (1983).

10) M. Kitano and K. Kuchitsu, *Bull. Chem. Soc. Jpn.*, **47**, 67 (1974).

11) J. Ladell and B. Post, *Acta Crystallogr.*, **7**, 559 (1954).

12) E. D. Stevens, *Acta Crystallogr.*, *Sect. B*, **34**, 544 (1978).

13) A. Pullman, H. Berthod, C. Giessner-Prettre, J. F. Hinton, and D. Harpool, *J. Am. Chem. Soc.*, **100**, 3991 (1978).

14) N. R. Carlsen, L. Random, N. V. Riggs, and W. R. Rodwell, *J. Am. Chem. Soc.*, **101**, 2233 (1979).

15) L. V. Vilkov, P. A. Akishin, and V. M. Presnyakova, *Zh. Strukt. Khim.*, **3**, 5 (1962); *J. Struct. Chem. USSR*, **3**, 3 (1962).

16) R. A. Elzaro, Ph. D. Thesis, Michigan State Univ., East Lansing, Mich., 1973, *Diss. Abstr.*, *Int. B*, **34** (3), 1052 (1973).

17) Y. Gobillon, P. Piret, and M. V. Meerssche, *Bull. Soc. Chim. Fr.*, **1962**, 551.

18) L. Brun and C.-I. Brändén, *Acta Crystallogr.*, **20**, 749 (1966).

19) P. A. Koz'min, A. S. Kotel'nikova, M. D. Surazhskaya, T. B. Larina, Sh. A. Bagirov, and T. V. Misailova, *Kood. Khim.*, **4**, 1557 (1978); *Sov. J. Cood. Chem.*, **4**, 1183 (1978).

20) B. M. Rode and T. Pontani, *Mh. Chemie*, **109**, 871 (1978); B. M. Rode and R. Fussenegger, *J. Chem. Soc., Faraday Trans. 2*, **71**, 1958 (1975).

21) G. Fini and P. Mirone, *J. Chem. Soc., Faraday Trans., 2*, **70**, 1776 (1974).

22) A. G. Whittaker and S. Siegel, *J. Chem. Phys.*, **42**, 3320 (1965).

23) R. C. Neuman, Jr., W. Snider, and V. Jonas, *J. Phys. Chem.*, **72**, 2469 (1968).

24) W. T. Raynes and M. A. Raza, *Mol. Phys.*, **20**, 339 (1971).

25) H.-J. Bittrich and D. Kirsch, *Z. Phys. Chem. (Leipzig)*, **257**, 403 (1976).

26) M. Rabinovitz and A. Pines, *J. Chem. Soc.*, *B*, **1968**, 1110.

27) H. Ohtaki, M. Maeda, and S. Ito, *Bull. Chem. Soc. Jpn.*, **47**, 2217 (1974).

28) G. Johansson and M. Sandström, *Chem. Scr.*, **4**, 195 (1973).

29) H. Ohtaki, T. Yamaguchi, and M. Maeda, *Bull. Chem. Soc. Jpn.*, **49**, 701 (1976).

30) W. E. Stewart and T. H. Siddall, III, *Chem. Rev.*, **70**, 517 (1970) and references therein.